PHYSICAL REVIEW B **80**, 180101(R) (2009)

Driving-induced crossover in the avalanche criticality of martensitic transitions

Eduard Vives,[1,*] Daniel Soto-Parra,[1,†] Lluís Mañosa,[1] Ricardo Romero,[2] and Antoni Planes[1]
[1]*Departament d'Estructura i Constituents de la Matèria, Facultat de Física, Universitat de Barcelona, Diagonal 647, E-08028 Barcelona, Catalonia, Spain*
[2]*IFIMAT, Universidad del Centro de la Provincia de Buenos Aires and CICPBA, Pinto 399, 7000 Tandil, Argentina*
(Received 17 August 2009; revised manuscript received 20 October 2009; published 17 November 2009)

An experimental study of the statistical distribution of acoustic emission avalanches in martensitic transitions is presented. The critical exponents characterizing the power-law distributions of avalanches are measured as a function of cycling under soft-driving (stress-driving) and hard-driving (strain-driving) procedures. Results provide experimental support for a recent theory based on a spin model that predicts a crossover from classical criticality in the soft-driving case to self-organized criticality in the hard-driving case.

DOI: 10.1103/PhysRevB.80.180101 PACS number(s): 64.60.av, 05.70.Jk, 64.60.My, 81.30.Kf

Many ferroic and multiferroic materials undergo first-order phase transitions, occurring through a sequence of discontinuous steps or avalanches of the order parameter. These avalanches are acknowledged to reflect the fact that when slowly driven, these systems relax from a (marginally stable) metastable state toward another metastable state with an associated energy dissipation responsible for hysteresis. Usually, since metastable minima are separated by very high-energy barriers, the transition kinetics is not dominated by thermal fluctuations (athermal behavior). The configuration of metastable minima is determined by the intrinsic distribution of disorder in the system. This yields a complex free-energy landscape that is at the origin of its properties: the noisy nature of the response to the driving field and mesoscale phase separation reflected in a multidomain structure.[1] Martensitic materials are typical examples of this class of systems. In these ferroelastic materials, avalanches are related to sudden changes in the local strain field, which give rise to the emission of high-frequency acoustic waves. The acoustic emission (AE) (Ref. 2) in ferroelastic systems is the analog of Barkhausen noise in magnetic materials, which is associated with sudden changes in the local magnetization.[3] In addition to magnetic and elastic systems, similar phenomenology has been reported in systems such as ferroelectrics[4] and superconductors.[5,6]

In all these systems, the distribution of avalanche size and duration approaches a power law when disorder is conveniently tuned. This reveals a tendency to reach a critical state characterized by the absence of size and duration characteristic scales of the avalanches. This criticality can be understood within the framework of lattice models with (different kinds of) quenched disorder following athermal dynamics that correspond to a local energy relaxation.[7] Due to this local character, the evolution of the system when driven by an external field will not, in general, follow an equilibrium path but rather evolve through metastable states. Since criticality is found for a given amount of disorder, one refers to it as disorder-induced criticality. In thermally induced martensitic transitions,[8] this has been checked by taking advantage of the fact that dislocations are formed during the transformation process and thus the amount of disorder can be controlled by cycling through the transition. Starting from a virgin sample (suitably heat treated), it has been shown that the distribution of the amplitudes of the acoustic signals (avalanches) evolves from supercritical to critical with the number of cycles.[9,10]

The driving mechanism has been argued to strongly influence the transition path.[11–15] The two important extreme driving situations consist of controlling either the externally applied field or its corresponding generalized displacement (thermodynamically conjugated variable). In the first case, driving is *soft* in the sense that displacement is free to fluctuate, while it is *hard* in the second case since displacement is constrained by the driving device. Recently, this problem has been theoretically addressed by Pérez-Reche *et al.*[16] The authors found a crossover between two different kinds of criticality determined by the mode of driving. When changing from soft to hard driving, criticality evolves from classical behavior requiring fine tuning of disorder to disorder-independent self-organized criticality. The exponents, characterizing the distribution of avalanche sizes, are higher for the soft case. The aim of the present Rapid Communication is to analyze the critical behavior during the stress-induced (soft-driving) and the strain-induced (hard-driving) martensitic transition in a Cu-Zn-Al single crystal and compare it with the results of the proposed theory.

In general, a reliable control of the generalized displacement (i.e., magnetization in magnetic systems or polarization in ferroelectrics) in the transition region, where systems display nonlinear behavior, is difficult. However, this is the common procedure in mechanical experiments performed with standard (screw-driven) tensile machines. In the present Rapid Communication, results obtained with this kind of hard device, which enables control of elongation, are compared to those obtained with a special soft machine that allows fine control of the applied force (external field), while the elongation is monitored.[19] In both cases, avalanches have been quantified from the AE generated during the martensitic transition.

The studied sample is a $Cu_{68.13}Zn_{15.74}Al_{16.13}$ single crystal that exhibits a cubic ($L2_1$) to monoclinic ($18R$) transition. In the absence of externally applied stress, the transition temperature is 234 K. The sample has cylindrical heads and a 35-mm (long) $\times$ 1.4-mm $\times$ 3.95 mm body. Prior to the sequence of studied load-unload cycles, an appropriate heat treatment was performed so that the sample was in the ordered state, free from internal stresses, and the vacancy

concentration was minimum at room temperature. Sample details and heat treatment can be found elsewhere.[15]

The two driving devices use the same sample grips, strain gauge, and load cell. The hard-driving machine is a commercial INSTRON 4302 that imposes a relative speed of the sample heads. The soft machine, especially designed,[15] controls an increasing/decreasing dead load hanging from the sample.

In out-of-equilibrium experiments, in which the sample evolves through a sequence of metastable states, it is well known that several factors may influence the transitions dynamics; among others, the number of cycles, loading/unloading rate, aging time between cycles, the exact limiting values of the driving parameter, etc. It is also very important that the contact between sample and grips is not altered during the experiments. For this reason, we have studied a sequence of 45 cycles in each setup without modifying the contact of the grips with the sample (i.e., never decreasing the force below 30 N). We have used the following protocol: after the heat treatment, three series of 10 cycles are performed at a low rate (0.31 N/s or 0.05 mm/min), an intermediate rate (0.42 N/s or 0.1 mm/min), and a high rate (0.82 N/s or 0.2 mm/min), followed by three series of 5 cycles at the same intermediate, high and low rates. In this Rapid Communication, we will focus only on the analysis of the forward transition from cubic to martensite.

In addition to the measurement of the applied load (accuracy of 0.5 N) and the sample deformation (accuracy of 0.02 mm), we have also detected AE signals by means of a PCI-2 system from Europhysical Acoustics working at 1 Msample/s. Two PZT transducers (micro-80) are used, coupled to the upper and lower grips that hold the sample. The contact of the sample with the grips and of the grips with the detectors is lubricated with vaseline in order to improve the signal transmission. The electric signals from the detectors are preamplified (40 dB) and input into the acquisition card. Electronics is adjusted so that a "hit" starts when the signal increases above a threshold of 42 dB and ends after more than 200 ms below threshold. For each hit, we measure the amplitude (in integer dB) defined as $A=20\log_{10}(V/1\ \mu\mathrm{V})-40$ dB, where V is the maximum voltage of the pulse and the absolute energy (in aJ), obtained by a fast time integration of the squared voltage of individual signals divided by the reference resistance of 10 kΩ.

The method of using two detectors allows for one-dimensional localization of the AE source. This enables electrical noise, signals coming from the contact with the grips or phenomena occurring in the sample heads, to be discarded. We consider as physical "events" only those which correspond to pairs of hits (one on each detector) separated by less than 0.038 ms. This is the upper bound time interval for a signal to cross the full length (35 mm) of the sample and has been obtained from a previous calibration.

The use of two detectors also allows for the estimation of the energy E_0 and amplitude A_0 of the event at the source point, which in general will be different from the amplitude and energy of the hits reaching the transducers. In previous thermally induced experiments,[17] since samples had dimensions typically smaller than the transducers, such a difference was not taken into account. In the present case, the effect must be taken into account given the length of the sample.

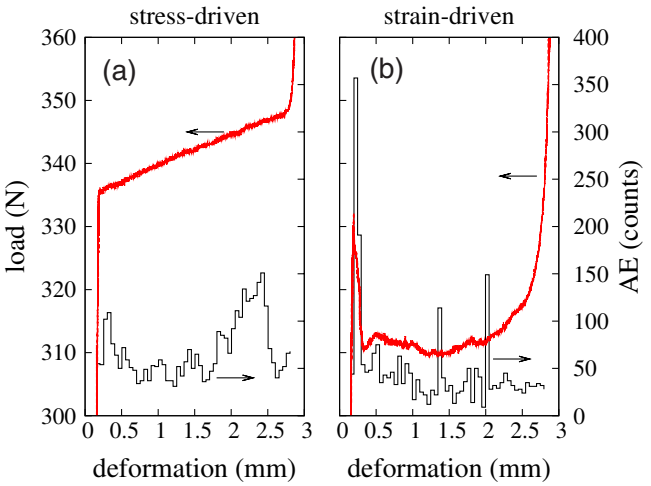

FIG. 1. (Color online) Comparison of the AE activity along stress-driven (a) and strain-driven (b) loading transitions. In both cases, data correspond to the fifth cycle after the heat treatment at rates 0.31 N/s and 0.05 mm/min. Histogram bin size for the AE activity is 0.05 mm

If $A_1(A_2)$ and $E_1(E_2)$ are the amplitude and energy detected by the transducer 1(2), one can estimate E_0 and A_0 from the following expressions:

$$A_0 = \frac{A_1 + A_2}{2}$$

$$E_0 = \sqrt{E_1 E_2}, \tag{1}$$

which assume that there is an average constant attenuation factor and they neglect additive constants on the amplitude and constant prefactors on the energy, which will not alter the measured properties of the statistical distribution.

Figure 1 shows, as an example, the comparison of the load versus elongation trajectories obtained by the two driving setups, corresponding to cycle number 5. As already studied in a recent paper,[15] the stress-driven curve displays linear behavior during the transition, whereas the strain-driven curve shows a yield point followed by strong fluctuations of the force. The AE activity (number of events per 0.05 mm deformation interval) is also very different. The strain-driven (hard) histogram (b) exhibits many peaks of AE activity, which in some cases can be correlated with strong fluctuations of the measured force. On the other hand, the stress-driven (soft) histogram (a) shows a much smoother AE activity, with a small increase at the beginning and end of the transition.

Figure 2 shows examples of the amplitude and energy distributions, corresponding to loop number 12, obtained with the two driving devices. As can be seen, above a certain cutoff, data exhibit a power-law distribution for almost 2 decades (40 dB) for amplitudes and 3 decades for energies. Note that the low amplitude and low-energy cutoffs are not sharp. This is a consequence of the fact that the 42 dB threshold is applied to the signals reaching the transducers close to the heads of the sample. Therefore, the threshold

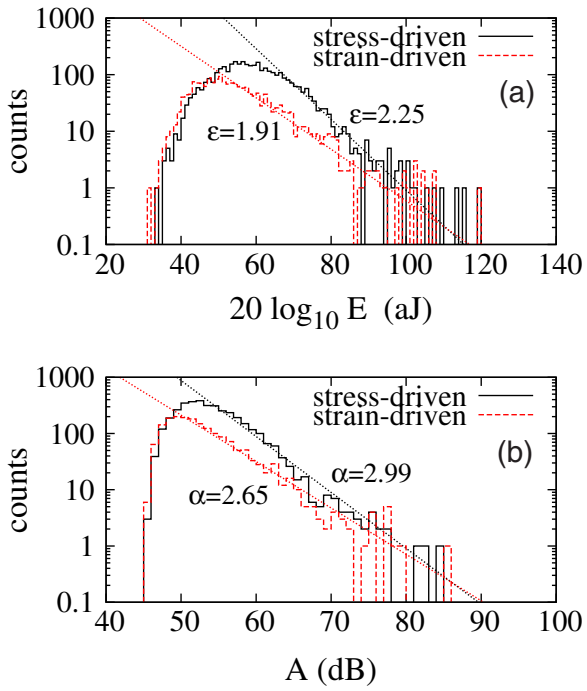

FIG. 2. (Color online) Example of energy (a) and amplitude (b) distributions for strain- and stress-driven loading transitions. Data correspond to the 12th cycle. Dotted straight lines show the behavior of the ML-fitted power-law distributions.

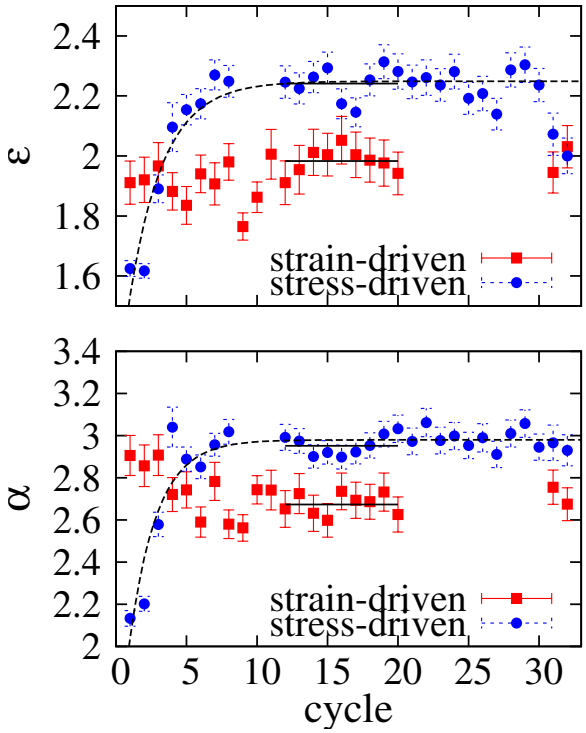

FIG. 3. (Color online) ML-fitted exponents ϵ and α as a function of the number of cycles for strain- and stress-driven cases. Dots correspond to stress-driven cycles and squares to strain-driven cycles. The dashed line shows the fitted exponential evolution and the continuous lines indicate the ML value obtained by the simultaneous fit of cycles 12–20.

represents a much larger cutoff for events occurring close to the heads than for signals occurring in the middle of the sample. This effect distorts the statistics in the low-energy and low-amplitude regions. The power-law exponents characterizing the probability densities $p(V) \sim V^{-\alpha}$ and $p(E) \sim E^{-\epsilon}$ can be obtained directly from the set of recorded amplitudes $\{A_{0_i}\}$ and energies $\{E_{0_i}\}$ by the maximum-likelihood (ML) method. The corresponding estimators are

$$\hat{\alpha} = 1 + 40 \log_{10}\left[1 + \frac{1}{2(\langle A_{0_i}\rangle - A_{\min})}\right], \tag{2}$$

$$\hat{\epsilon} = 1 + \frac{1}{\langle \ln E_{0_i}\rangle - \ln E_{\min}}, \tag{3}$$

where $\langle\cdot\rangle$ denotes averages and $A_{\min}$ and $E_{\min}$ are the lower cutoffs for the fits. Note that the first formula takes into account the fact that amplitudes are not continuous but semi-integers. As an example of the fits, for loop number 12 shown in Fig. 2, one obtains $\hat{\epsilon}=2.25\pm0.05$ and $\hat{\alpha}=2.99\pm0.06$ for the stress-driven case and $\hat{\epsilon}=1.91\pm0.07$ and $\hat{\alpha}=2.65\pm0.08$ for the strain-driven case, which correspond to the behavior indicated by dashed lines in Fig. 2. The fitted values are stable when $A_{\min}$ is varied between 50 and 70 dB and $E_{\min}$ is varied between 1000 and 100 000 aJ.

Figure 3 shows the fitted exponents for cycles from 1 to 32 using $E_{\min}=3000$ aJ and $A_{\min}=55$ dB. The first interesting feature to mention is that in all cases, the values of the exponents tend to stabilize when increasing the number of cycles. This is the expected behavior for thermal cycling.[9,17] For the stress-driven case, we find that such a stabilization is approximately exponential (as indicated by the fit in Fig. 3) and requires the first 6 to 7 cycles. For the strain-driven case (taking into account the error bars), data seem to indicate that the exponents do not depend on the cycle number: already from the first loop, avalanches distribute with the same power-law exponent. This is particularly clear for the exponent ϵ.

A second interesting comment is that, after stabilization, exponents do not depend on the driving rate (in the studied ranges). Note that data from cycle 1 to 10 correspond to the low driving rate, data from cycle 11 to 20 to the intermediate driving rate, and from cycle 21 to 30 to the fast driving rate.

The third point to be made is that the exponents for the stress-driven case (soft-driving) are larger than exponents for the strain-driven case (hard driving). In order to get a good

TABLE I. Summary of the fitted exponents ϵ and α, corresponding to the accumulated data for loops 12 to 20. The third column indicates the theoretical values proposed in Ref. 16. Note that this exponent corresponds to the distribution of avalanche sizes but not to avalanche energies.

Driving	ϵ	α	τ (theory[a])
Soft (stress-driven)	2.24 ± 0.02	2.95 ± 0.02	1.6 ± 0.06
Hard (strain-driven)	1.98 ± 0.03	2.67 ± 0.03	1.3 ± 0.06

[a]Reference 16.

estimation for the numerical values of the exponents, we have fitted the data in loops 12–20 (all correspond to the same intermediate driving rates) with the ML method. The fitted values are summarized in Table I. For the sake of comparison, we also give the theoretical exponent τ corresponding to the power-law distribution of avalanche sizes (number of spins flipped during the avalanche) in Ref. 16.

Note that the value $\alpha \sim 3$ for the stress-driven case is in very good agreement with the thermal exponents for alloys with a very similar composition, transforming from cubic to 18*R*. This indicates that the microscopic avalanche dynamics is very similar for the two unconstrained situations (soft driving) and thermal driving, although in the first case the system transforms to a single variant of martensite and in the second case to a multivariant structure.

When comparing our results to theoretical predictions,[16] it should be noted that our data agree with two important facts. First the exponents for the soft-driving case are larger (there are relatively more small avalanches compared to large avalanches). Second, the exponents for the hard-driving case do not show an evolution to a final stable value but seem to be already stable from the first loops. The quantitative comparison of the exponents with theoretical predictions is, however, difficult since it is not clear what the exact relation between the energy and amplitude of the AE pulses is with the energy released, size, or duration of the avalanches. A dynamical theory for the understanding of the generation of AE events during martensitic transitions is still lacking.[18]

Agreement with the two predictions strongly supports the hypothesis that in the hard-driving case, the interfaces that move during the transition self-organize into a critical dynamical behavior irrespective of the amount of disorder. For the soft-driving case, only by tuning the disorder does one reach the final critical state. This tuning of the disorder in our case is obtained only after the first 6 to 7 cycles. The mechanism for such a tuning of disorder when cycling has also been theoretically explained recently with a model that considers the role of dislocations during the martensitic transition.[10]

This work received financial support from CICyT (Spain) through Project No. MAT2007-61200 and from the E.U. through Marie Curie through Grant No. MRTN-CT-2004-505226 RTN MULTIMAT.

*eduard@ecm.ub.es

†Permanent address: Centro de Investigación en Materiales Avanzados S.C. Miguel de Cervantes 120, Complejo industrial Chihuahua, 31109 Chihuahua, México.

[1] T. Castán, Ll. Mañosa, E. Vives, A. Planes, and A. Saxena, in *Magnetism and Structure in Functional Materials*, edited by A. Planes, Ll. Mañosa and A. Saxena (Springer-Verlag, Berlin, 2005), pp. 27–48.

[2] C. B. Scruby, J. Phys. E **20**, 946 (1987).

[3] G. Durin and S. Zapperi, in *The Science of Hysteresis*, edited by G. Bertotti and I. D. Mayergoyz (Elsevier, Amsterdam, 2005), Vol. II, pp. 130–267.

[4] M. Roth, E. Mojaev, E. Dul'kin, P. Gemeiner, and B. Dkhil, Phys. Rev. Lett. **98**, 265701 (2007).

[5] W. Wu and P. W. Adams, Phys. Rev. Lett. **74**, 610 (1995).

[6] S. Field, J. Witt, F. Nori, and X. Ling, Phys. Rev. Lett. **74**, 1206 (1995).

[7] J. P. Sethna, K. A. Dahmen, and C. R. Myers, Nature (London) **410**, 242 (2001).

[8] In this case, the transition is driven by slowly cooling/heating in the absence of any field, breaking the low-temperature phase degeneracy.

[9] F. J. Pérez-Reche, M. Stipcich, E. Vives, L. Mañosa, A. Planes, and M. Morin, Phys. Rev. B **69**, 064101 (2004).

[10] F. J. Pérez-Reche, L. Truskinovsky, and G. Zanzotto, Phys. Rev. Lett. **99**, 075501 (2007).

[11] J. L. Ericksen, J. Elast. **5**, 191 (1975).

[12] G. Puglisi and L. Truskinovsky, J. Mech. Phys. Solids **48**, 1 (2000).

[13] X. Illa, M. L. Rosinberg, and E. Vives, Phys. Rev. B **74**, 224403 (2006).

[14] X. Illa, M. L. Rosinberg, P. Shukla, and E. Vives, Phys. Rev. B **74**, 224404 (2006).

[15] E. Bonnot, R. Romero, X. Illa, Ll. Mañosa, A. Planes, and E. Vives, Phys. Rev. B **76**, 064105 (2007).

[16] F. J. Pérez-Reche, L. Truskinovsky, and G. Zanzotto, Phys. Rev. Lett. **101**, 230601 (2008).

[17] Ll. Carrillo, L. Mañosa, J. Ortín, A. Planes, and E. Vives, Phys. Rev. Lett. **81**, 1889 (1998).

[18] An interesting preliminary attempt based on Lagrangian dynamics can be found in Oguz Umut Salman, Ph.D. dissertation, Universite Pierre et Marie Curie, Paris, 2009.

[19] To refer to the two studied driving mechanisms, we will use the words *stress driven* and *strain driven*, although strictly speaking it would be more precise to use *force driven* and *elongation driven*.